Int. J. Electrochem. Sci., 15 **(2020)** 3232 – 3241, doi: 10.20964/2020.04.21

International Journal of
ELECTROCHEMICAL
SCIENCE
www.electrochemsci.org

Threshold Level of Chloride Ions for Corrosion of SD345 Carbon Steel Reinforcement in Concrete

Yujie Wang, Hui Zhou[*]*, Youheng Zhang*

Department of Architectural Engineering, North China Institute of Aerospace Engineering, Hebei, China Langfang 065000, China
[*]E-mail: lfzhouhuihui@sina.com

Received: 16 November 2019 / *Accepted:* 26 January 2020 / *Published:* 10 March 2020

Reinforced concrete is one of the most commonly used materials in the construction industry. The most and main causes of reinforcement corrosion in concrete structures are chloride attack and carbonation. Many studies have been carried out in this field so far, but due to the multitude of influencing factors and their complexity, different results have been obtained. In this study, reinforced concrete samples were prepared and investigated to monitor the threshold of chloride concentration for corrosion of SD345 carbon steel rebar using the electrochemical impedance spectroscopy (EIS) and half-cell potential (HCP) tests. A series of electrolyte solutions containing different NaCl contents, that is, 0, 1, 2 and 3 wt%, were used to simulate the chloride environment. Given that the HCP values are relatively low for carbon steel rebars, there are a high possibility for corrosion of all samples. By increasing the NaCl content in electrolyte solution, the current density values were increased from the early stages, indicating corrosion enhancement in the samples with increasing chloride ions in solution. The EIS results show that resistance of passive film gradually decreased by increasing the chloride concentration which shows that non-protective corrosion and porous products have been advanced on the surface of steel rebar. Furthermore, the EIS findings indicated an obviously increase of charge transfer resistance and a clearly reduction in the non-ideal interfacial capacitance after 16 weeks exposed to 2 wt% NaCl solution which can be attributed to the high degree of hydration and the efficiently refined the pore structure of the reinforced concretes. Scanning electron microscopy analysis confirmed the results obtained by electrochemical experiments.

Keywords: SD345 carbon steel rebar; Corrosion resistance; Electrochemical study; Threshold level of chloride ions; Half-cell potential

1. INTRODUCTION

Reinforced concrete structures are subject to corrosion in severe marine environments [1]. The process of corrosion in steel reinforced concrete is due to the penetrations of aggressive species like chloride ions [2, 3]. Chloride-induced corrosion in steel rebar is one of the most important causes of

deterioration leading that results in reduced service life of reinforcement steel structures [4]. The chloride ions cause the breakdown of passive film at the concrete-steel interface even at high level of pH [5]. The corrosion rate depends on the presence of water and oxygen near the interface [6].

The corrosion initiation time is affected by concrete cover and the critical concentrations of chloride [7]. Furthermore, the cement paste porosity directly influences the diffusivity of concrete. Prediction and estimation models are existent in the literature to help scientists and engineers in predicting the efficiency of reinforced concrete bridges, buildings and other structures exposed in the severe marine environment [8-10]. The continuous hydration of cement changes the structure of the concrete and leads to the decrease of the chloride ions penetration in prolonged periods [11]. Thus, properties of time-dependent must be studied in evaluating and predicting durability of concrete [12, 13].

Many studies have been done to evaluate the chloride influence on the corrosion activities of steel reinforced concrete [14, 15]. Traditional methods in determining the threshold Levels of chloride ions are generally based on the measurement of chloride ion content in the system. Given the deterioration and difficulty of traditional methods, the need to develop easy and optimal alternatives is increasingly felt. Electrochemical tests such as electrochemical impedance spectroscopy (EIS) are conventionally used to characterize electrochemical reactions and ionic transport [16, 17]. This method can be utilized to estimate the electrical properties of reinforcement steel rebar during the exposure process and helping on the measurement of the polarization resistance and the corrosion potential of the steel rebar when exposed to the chloride ions. Half-cell potential measurement is suitable in determining the corrosion behavior of steel rebar [18, 19]. Therefore, in present study, the EIS and Half-cell potential tests were used to investigate the success rate of electrochemical methods in determining the system state with respect to the threshold of chloride ion. Moreover, the accuracy of the results of these tests was discussed using scanning electron microscopy.

2. MATERIALS AND METHODS

100 mm long cylindrical concrete samples with the width of 50 mm and a 10 mm diameter steel rod embedded in their centers were made. Chemical cleaning was done on the steel surface before using. The chemical composites of SD345 carbon steel rebar are listed in Table 1. Table 2 presents the chemical composition of the common Portland cement used. Cardboard molds were used to form the specimens and then placed in a room at 20 ºC with no humidity for a day.

Table 1. The chemical compositions of SD345 carbon steel rebar (wt%)

Si	Mn	S	P	N	C	Cr	Fe
0.31	1.34	0.02	0.029	0.005	0.22	0.084	Bal.

After removing the mold, the samples were kept in a wet room at 20 ± 1 ºC and 100% relative humidity for 28 days and then exposed to contact with NaCl solution for the first time. A series of

electrolyte solutions containing different NaCl contents, that is, 0, 1, 2 and 3 wt%, were used to simulate the chloride environment. All the solutions employed in the test were prepared using analytical reagents and double DI water. All electrochemical experiments were done in a three-electrode system at room temperature. The reinforcement carbon steel electrode, saturated calomel electrode and Pt foil were utilized as the working electrode, reference electrode and counter electrode, respectively. The EIS measurements were performed in a frequency ranging from 0.01 Hz to10^5 Hz. The corrosion potential of steel rebars was calculated by means of half-cell potential (HCP) measurement. The HCP value indicates the probability of corrosion activity of the reinforcing steel located beneath the half-cell, as described by ASTM C-876. The setup basically consisted of an external copper/ copper sulfate electrode (CSE), connecting wires and a high impedance voltmeter. The HCP measurement has been widely used in the field due to its simplicity and general agreement among researchers that it effectively indicates the probability of active corrosion along the steel reinforcement in concrete. Macrocell corrosion current is a good indicator of corrosion initiation of the steel rebar. Corrosion current (I) was measured indirectly as a voltage drop across the resistor connected externally between the top and bottom steel rebar. The corrosion current was determined based on Ohm's law as indicated in Eq (1).

$$V = IR \quad (1)$$

where I is the current (μA), V is the voltage drop across the resistor (μV), R is the electrical resistance. A high impedance voltmeter with a resolution of 0.01 mV is recommended by ASTM G109. Then, corrosion current density (i_{corr}) was measured as shown in Eq (2).

$$i_{corr} = I/A \quad (2)$$

where i_{corr} is the corrosion current density (μA/cm^2), and A is the surface area of exposed reinforcing steel. The surface morphology of the samples was characterized by scanning electron microscopy (SEM, JEOL JSM-7600F).

Table 2. Chemical composition of the Portland cement

Compositions	Contents (wt%)
CaO	62.8
SiO_2	21.8
Al_2O_3	4.7
Fe_2O_3	2
MgO	2
SO_3	3.8
LoI	1.8

3. RESULTS AND DISCUSSION

The corrosion possibility of SD345 carbon steel reinforced concrete was considered by the potential of the reinforcement steel using HCP technique. As shown in figure 1, there is a high possibility of corrosion of the steel rebars because the HCP values are relatively low. Table 3 shows the

classification criteria derived from ASTM-C876 standard. The principle included in this method was fundamentally corrosion potential measurement of steel rebar with regard to a CSE [20].

Table 3. Range of half-cell corrosion potential related to the probability of corrosion given by ASTM-C876

Corrosion potential (mV vs. CSE)	Probability of corrosion
< -350	90%
-350 to -200	Uncertain
> -200	10%

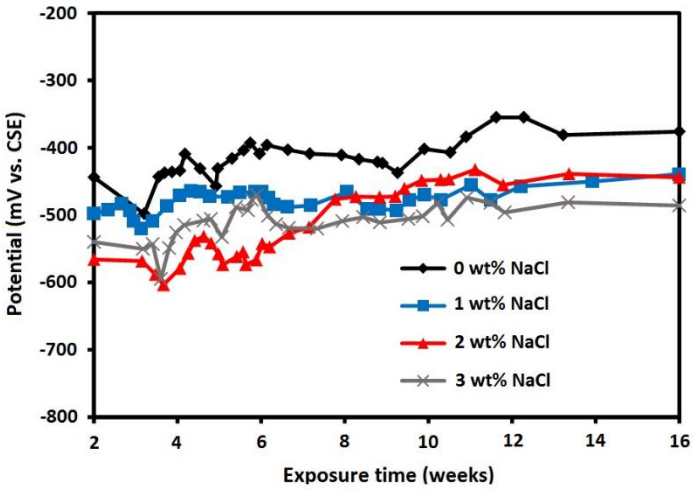

Figure 1. Half-cell potential of the SD345 carbon steel reinforced concrete immersed in different concentrations of NaCl

As shown in figure 1, for the sample immersed in salt-free distilled water, the potential value reduced with the increase in the exposure time. Due to the absence of chloride ions in the test environment, the potential increase cannot be related to the passivation layer on the steel rebar. Water-saturated concrete and gradually increase of reinforced concrete potential with increase of time can introduce an increase in oxygen concentration causing the rebar potential to enhance. The oxygen concentration in saturated concrete usually enhances the potential of reinforced concrete to more positive values. The potential of the samples at the beginning of the immersion in NaCl solution is less than -350 mV, which indicates a relatively intense corrosion. But it should be noted that this potential only indicates the possibility of corrosion. Also, as noted in the ASTM-C876 standard, the threshold value of -350 mV corrosion potential versus a $Cu/CuSO_4$ for water-saturated concrete does not apply [21]. The reason for this phenomenon is the restriction of oxygen penetration in the water-saturated concrete and consequently the inability to form a protective layer. On the other hand, the occurrence of corrosion depends on the cathodic reaction and the possible cathodic reaction in the reinforced concrete system requires oxygen, which leads to a decrease in the corrosion rate. Furthermore, the existence of high

resistance layers can affect the potential. When the layers of corrosion products are formed on the surface of steel rebar, this potential difference can occur. The difference due to the distance of rebar from the reference electrode can be reduced by using a permanent reference electrode within concrete [22].

Figure 2 shows the measurement of macrocell corrosion current density by the AC impedance technique according to polarization resistance in the samples. According to classification criteria for the corrosion current density [23], all samples are in low corrosion state during exposure time**.** With the increase the NaCl content in electrolyte solution, the current density values were increased from the early stages, indicating corrosion enhancement in the samples with the increase of chloride ions in the solution. Furthermore, in every sample with increasing exposure time, the corrosion current density was reduced. These findings were consistent with the HCP results.

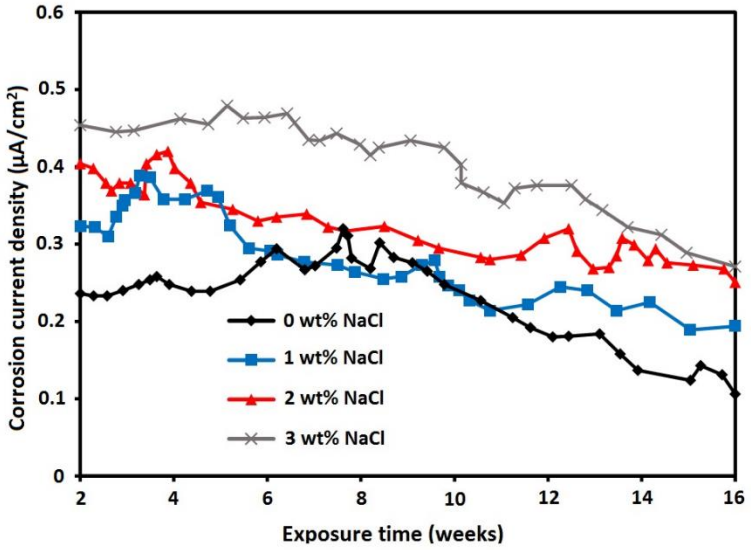

Figure 2. Corrosion current density of the SD345 carbon steel reinforced concrete immersed in different concentrations of NaCl

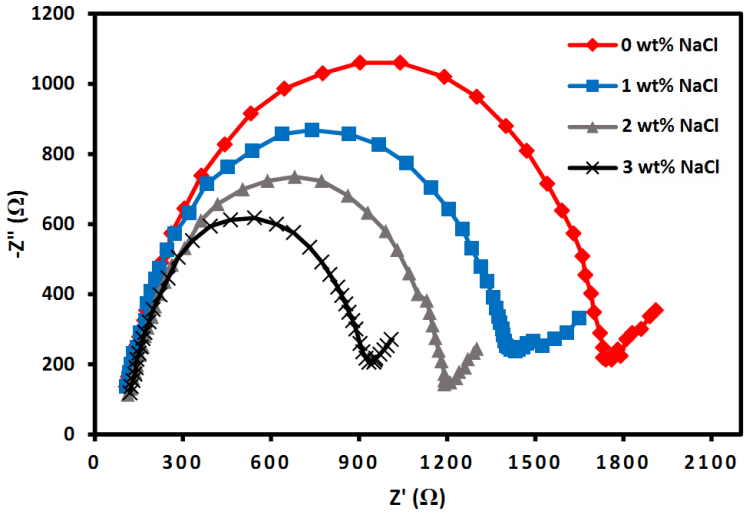

Figure 3. EIS diagrams of the SD345 carbon steel reinforced concrete immersed into the electrolyte solution with different concentration of NaCl after 2 weeks exposure time

In order to examine the corrosion behavior of the steel rebar, the EIS measurements were carried out. The Nyquist diagrams of the steel rebars immersed in different concentrations of NaCl solution are shown in Figure 3. Nyquist plots typically indicate a capacitive loop where the diameter of loops are reducing with the increase of NaCl content. It can be attributed to the corrosion behavior of chloride ions on the surface of steel. John et al. [24] offered a circuit model for calculating corrosion rate in reinforced concrete specimens, where the EIS plot at the high-frequency is associated to the resistance between the working electrode and the electrolyte solution. Moreover, the EIS diagram at the low-frequency can be associated to the charge transfer resistance in the corrosion procedure [25]. Figure 4 indicates an equivalent circuit with two time constants which suggested to simulate the electrochemical procedure of steel rebars used by other researchers. R_m is the mortar resistance which correspond to the high-frequency response. Since, the resistance of electrolyte was insignificant compared to the resistance of mortar in this study, the electrolyte resistance was therefore neglected. During the passivity process, the parameters of second time constant observed at the low frequencies such as R_{ct} and C_{dl} were ascribed to the charge transfer resistance and non-ideal interfacial capacitance of the steel surface [26]. It indicated that the corrosion protection of the steel rebar was controlled by the passive film properties [27]. The parameters of first time constant observed at the low frequencies such as R_f and C_f were attributed to the redox transformation in the corrosion products which happened on the oxide film surface.

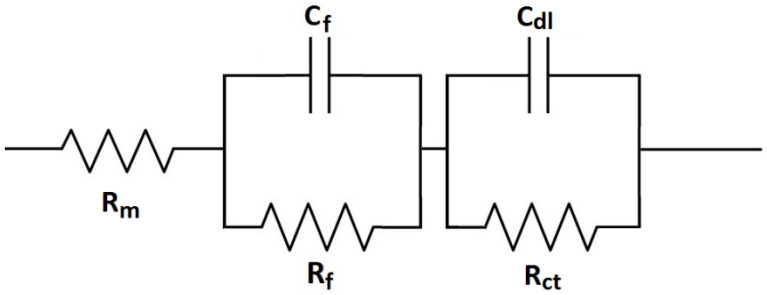

Figure 4. An equivalent circuit model to fit the experimental data

The best fitting elements based on the electrical circuit revealed in figure 4 are listed in Table 3. As shown, the R_{ct} value significantly reduced from 1795 Ω to 978 Ω, by adding a small amount of NaCl in the electrolyte solution, indicating that the NaCl presence had led to an enhanced corrosion on the steel surface.

Table 3. Electrochemical parameters from the fitting using the equivalent circuit in Figure 3 for different concentration of NaCl in electrolyte solution

NaCl concentration	R_m (Ω)	R_f (Ω)	C_f (μF cm^{-2})	R_{ct} (Ω)	C_{dl} (μF cm^{-2})
0 wt%	78	1134	1.1	1795	1.8
1 wt%	65	893	2.8	1486	3.7
2 wt%	49	686	3.7	1205	4.6
3 wt%	62	457	4.5	978	5.9

Furthermore, table 3 indicates that R_f gradually decrease by increasing the chloride concentration which shows that non-protective corrosion and porous products had been advanced on the surface of steel rebar. These results are in accordance with the best fitting findings for C_{dl} which were steadily increasing over 5.9 μFcm^{-2} with 3 wt% NaCl in the electrolyte solution, demonstrating that generalized corrosion may occur on the surface of steel rebar [28]. This phenomenon can be clarified that the passive layer on the surface of steel rebar was an unbroken protective layer once the chloride concentration was less than the value of threshold [29]. However, by increasing the chloride content, the passive layer became local and unstable breakdown, and the pitting corrosion appeared at some location of the steel surface [30].

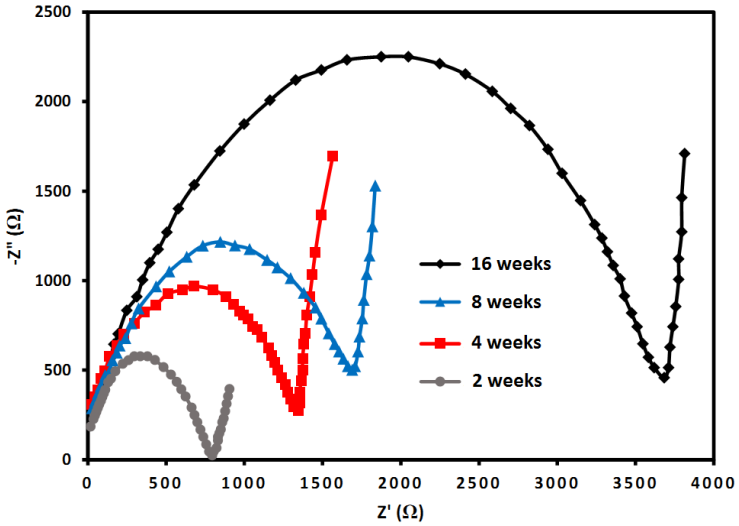

Figure 5. EIS diagrams of the SD345 carbon steel reinforced concrete immersed into 2 wt% NaCl solution with different exposure time

Table 3. Electrochemical parameters from the fitting using the equivalent circuit in Figure 5 for different exposure times in 2 wt% NaCl solution

Exposure time (week)	R_m (Ω)	R_f (Ω)	C_f (μF cm^{-2})	R_{ct} (Ω)	C_{dl} (μF cm^{-2})
2	3.4	932	4.3	820	5.6
4	4.5	985	3.9	1470	4.9
8	5.8	1102	4.1	1953	4.5
16	7.5	1174	4.2	3840	2.3

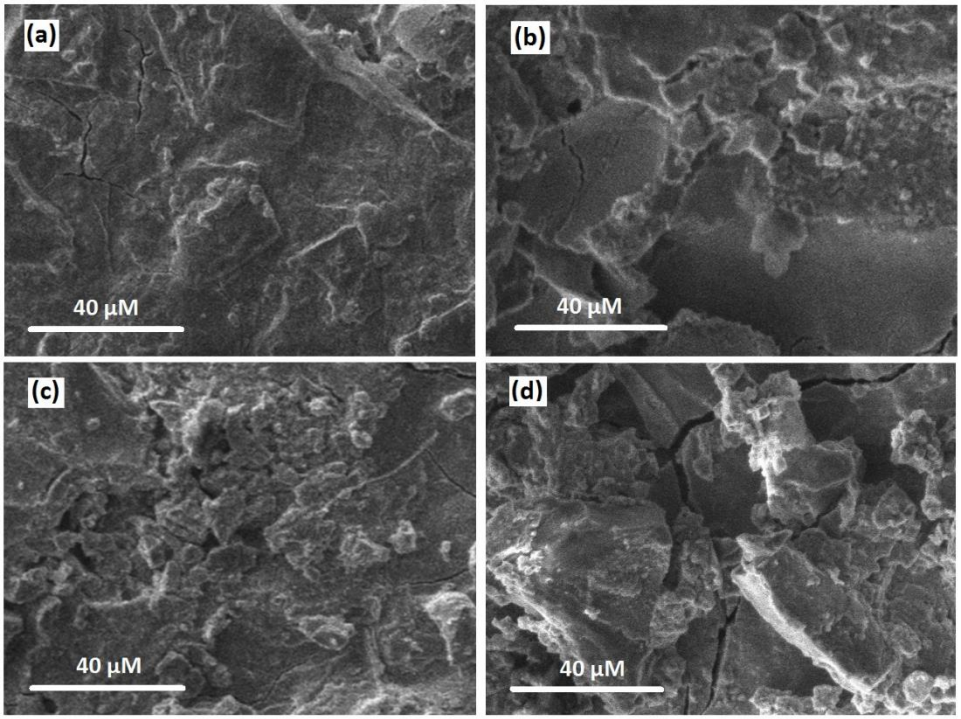

Figure 6. The SEM images of SD345 carbon steel rebars after 8 weeks immersion electrolyte solution with different NaCl concentrations (a) 0 wt% (b) 1 wt% (c) 2 wt% and (d) 3 wt%.

Figure 5 shows Nyquist plots of the samples immersed into 2 wt% NaCl solution with different exposure time. The best fitting elements based on the electrical circuit revealed in figure 4 are listed in Table 4. Results indicate that the R_{ct} increased about 4.5 times from 2 to 16 weeks exposure time, with a reduction in the C_{dl} from 5.6 to 2.3 µF cm^{-2}, possibly due to hydration products having a higher density and the efficiently refined the pore structure of the reinforced concretes in 16 weeks exposure time. Bragança et al. [31] reported comparable behavior, with a reduction in capacitance. Furthermore, the concrete resistance doubled after 16 weeks compared to 2 weeks exposure time which can be attributed to the pore size refinement, tortuosity and distribution of capillary pores and also chemical interactions between cement compounds and adsorbed ions [32]. Moreover, The C_f remained stable for all exposure time, demonstrating no degradation in the protective oxide layer on the steel rebar, as expected for a limited immersion time.

To study the corrosion behavior of steel rebar in electrolyte solution with different NaCl concentrations, the surface morphology of the reinforcement steel after 8 weeks immersion were done by SEM. Figure 6a indicates the SEM image of the sample surface immersed in the salt-free distilled water solution. As shown, no corrosion pits appeared on the surface. However, some mechanical scratches resulting from the polishing process appeared on the steel surface. When the NaCl concentration was up to 1 wt%, some tiny pits appeared on the steel surface (Figure 6b), indicating the corrosion process happened at some location. With the increase of the NaCl concentration, some larger corrosion and pits were deposited on the surface of the steel rebar (Figure 6c and d). All these observations were in good agreement with the results of the obtained electrochemical measurements.

4. CONCLUSIONS

In this study, SD345 carbon steel reinforced concrete samples were prepared to investigate the threshold of chloride concentration for corrosion of rebar using the EIS and HCP tests. A series of electrolyte solutions containing different NaCl contents, that is, 0, 1, 2 and 3 wt%, were used to simulate the chloride environment. By increasing the NaCl content in electrolyte solution, the current density values were increased from the early stages, indicating corrosion enhancement in the samples with increasing chloride ions in the solution. The EIS results show that R_f gradually decreased by increasing the chloride concentration which shows that non-protective corrosion and porous products have been advanced on the surface of the steel rebar. Furthermore, the EIS findings indicated an obviously increase of R_{ct} and a clearly reduction in the C_{dl} after 16 weeks exposure to 2 wt% NaCl solution which can be attributed to the high degree of hydration and the efficiently refined of the pore structures of the reinforced concretes. A reduction in the overall impedance values with increasing concentration of NaCl reveals a decrease of the corrosion resistance. Scanning electron microscopy observations were in good agreement with the results of obtained electrochemical measurements.

ACKNOWLEDGEMENTS:
This research was supported by Spatial Distribution Characteristics and Driving Factors of Roads in Langfang City Based on GIS, Science and technology research and development plan of Langfang City, China (Grant No. 2016011080) and Analysis of Road Distribution and Driving Factors in Langfang City under the Integration of Beijing, Tianjin and Hebei, Research Fund Project of North China Institute of Aerospace Engineering, China (Grant No. KY-2016-13)".

References

1. S. Kakooei, H.M. Akil, M. Jamshidi and J. Rouhi, *Construction and Building Materials*, 27 (2012) 73.
2. H. Chen, S. Zhang, Z. Zhao, M. Liu and Q. Zhang, *Progress in Chemistry*, 31 (2019) 571.
3. D. Yuan, C. Zhang, S. Tang, X. Li, J. Tang, Y. Rao, Z. Wang and Q. Zhang, *Water research*, 163 (2019) 114861.
4. P. Castaldo, B. Palazzo and A. Mariniello, *Engineering Structures*, 130 (2017) 261.
5. S. Tang, N. Li, D. Yuan, J. Tang, X. Li, C. Zhang and Y. Rao, *Chemosphere*, 234 (2019) 658.
6. V. Volpi-León, L. López-Léon, J. Hernández-Ávila, M. Baltazar-Zamora, F. Olguín-Coca and A. López-León, *International Journal of Electrochemical Science*, 12 (2017) 22.
7. P. Shao, J. Tian, F. Yang, X. Duan, S. Gao, W. Shi, X. Luo, F. Cui, S. Luo and S. Wang, *Advanced Functional Materials*, 28 (2018) 1705295.
8. L. Peng and M.G. Stewart, *Structure and Infrastructure Engineering*, 12 (2016) 499.
9. C.K. Chiu, F.J. Tu and F.P. Hsiao, *Structure and Infrastructure Engineering*, 11 (2015) 345.
10. X. He, F. Deng, T. Shen, L. Yang, D. Chen, J. Luo, X. Luo, X. Min and F. Wang, *Journal of colloid and interface science*, 539 (2019) 223.
11. C. Li, S. Hu, L. Yang, J. Fan, Z. Yao, Y. Zhang, G. Shao and J. Hu, *Chemistry–An Asian Journal*, 10 (2015) 2733.
12. W. Zhu, S. Setunge, N. Gamage, R. Gravina and S. Venkatesan, *Journal of Performance of Constructed Facilities*, 31 (2017) 04017005.
13. L. Yang, G. Yi, Y. Hou, H. Cheng, X. Luo, S.G. Pavlostathis, S. Luo and A. Wang, *Biosensors and Bioelectronics*, 141 (2019) 111444.

14. F. Shaheen and B. Pradhan, *Cement and Concrete Research*, 91 (2017) 73.
15. P. Shao, J. Tian, X. Duan, Y. Yang, W. Shi, X. Luo, F. Cui, S. Luo and S. Wang, *Chemical Engineering Journal*, 359 (2019) 79.
16. J. Huang and A. Wang, *International Journal of Electrochemical Science*, 11 (2016) 4667.
17. P. Shao, L. Ding, J. Luo, Y. Luo, D. You, Q. Zhang and X. Luo, *ACS applied materials & interfaces*, 11 (2019) 29736.
18. M. Jin, S. Gao, L. Jiang, Y. Jiang, D. Wu, R. Song, Y. Wu and J. He, *Int. J. Electrochem. Sci*, 13 (2018) 719.
19. P. Shao, X. Duan, J. Xu, J. Tian, W. Shi, S. Gao, M. Xu, F. Cui and S. Wang, *Journal of hazardous materials*, 322 (2017) 532.
20. Y. Ji, Y. Hu, L. Zhang and Z. Bao, *Cement and Concrete Composites*, 69 (2016) 28.
21. N. Naderi, M. Hashim and J. Rouhi, *International Journal of Electrochemical Science*, 7 (2012) 8481.
22. M. Montemor, A. Simoes and M. Ferreira, *Cement and Concrete Composites*, 25 (2003) 491.
23. P. Rodriguez, E. Ramirez and J. Gonzalez, *Magazine of Concrete Research*, 46 (1994) 81.
24. D. John, P. Searson and J. Dawson, *British Corrosion Journal*, 16 (1981) 102.
25. J. Rouhi, S. Kakooei, M.C. Ismail, R. Karimzadeh and M.R. Mahmood, *International Journal of Electrochemical Science*, 12 (2017) 9933.
26. F. Husairi, J. Rouhi, K. Eswar, C.R. Ooi, M. Rusop and S. Abdullah, *Sensors and Actuators A: Physical*, 236 (2015) 11.
27. H.-S. Ryu, J.K. Singh, H.-S. Lee, M.A. Ismail and W.-J. Park, *Construction and Building Materials*, 133 (2017) 387.
28. K. Tang, *Corrosion Science*, 152 (2019) 153.
29. F. Husairi, J. Rouhi, K. Eswar, A. Zainurul, M. Rusop and S. Abdullah, *Applied Physics A*, 116 (2014) 2119.
30. D. Sazou, M. Pavlidou and M. Pagitsas, *Journal of Electroanalytical Chemistry*, 675 (2012) 54.
31. M.O. Bragança, K.F. Portella, M.M. Bonato and C.E. Marino, *Construction and Building Materials*, 68 (2014) 650.
32. P. Gu, P. Xie, J.J. Beaudoin and R. Brousseau, *Cement and Concrete Research*, 23 (1993) 157.